

32. (a) Shaik, S. S. *Prog. Phys. Org. Chem.* **1985**, *15*, 797.
 (b) McLennon, D. Pross, A. *J. Chem. Soc. Perkin Trans. 2*, **1984**, 981. (c) Carrion, F.; Dewar, M. J. S. *J. Am. Chem.*

- Soc.* **1984**, *106*, 3531. (d) Bach, R. D.; Coddens, B. A.; Wolber, G. J. *J. Org. Chem.* **1986**, *51*, 1030.

Synthesis and Reaction Chemistry of Some Ferrocene-Containing Chelate Ligands with Dirhodium Acetate: X-ray Crystal Structure of $(\eta^1\text{-}(S,R)\text{-CPFA})_2\text{Rh}_2(\text{OAc})_4$

Eun-Jin Kim and Tae-Jeong Kim*

Department of Industrial Chemistry, Kyungpook National University, Taegu 702-701, Korea

Received August 10, 1994

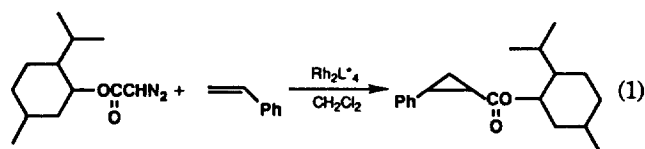
New ferrocene-based chelate amines, $\text{Fe}[\text{C}_5\text{H}_4\text{CH}(\text{Me})\text{NMe}_2]_2$ (**3**), $\text{Fe}[\text{C}_5\text{H}_3(\text{CH}(\text{Me})\text{NMe}_2)(\text{PPh}_2)\text{-}1,2]_2$ (**4**), $(\text{C}_5\text{H}_5)\text{Fe}(\text{C}_5\text{H}_3(\text{CH}_2\text{NMe}_2)(\text{CH}(\text{CN})\text{NMe}_2)\text{-}1,2)$ (**6**), and $(\text{C}_5\text{H}_5)\text{Fe}(\text{C}_5\text{H}_3(\text{CH}_2\text{NMe}_2)(\text{CH}(\text{Me})\text{NMe}_2)\text{-}1,2)$ (**7**) have been prepared. The reaction and the coordination chemistry of **4** and other related compounds (*S,R*)-(1-*N,N*-dimethylaminoethyl)-2-dicyclohexylphosphinoferrocene (CPFA) and 1,1'-bis-(diphenylphosphino)ferrocene (BPPF) with $\text{Rh}_2(\text{OAc})_4(\text{MeOH})_2$ were investigated. The reaction of the chiral ligand (*S,R*)-CPFA forms a complex of the type $(\eta^1\text{-}(S,R)\text{-CPFA-P})_2\text{Rh}_2(\text{OAc})_4$ (**8**) in which the ligand is coordinated to both rhodium centers in a monodentate fashion through phosphorus. In contrast, the bisphosphine analogues such as BPPF and **4** afford chelate complexes of the type $(\eta^2\text{-PP})\text{Rh}_2(\text{OAc})_4$ (**9** & **10**) where both ligands act as a chelate bidentate to a single rhodium atom. All these complexes were characterized by microanalytical and spectroscopic techniques. In one case, the structure of **8** was determined by X-ray crystallography. Crystals are monoclinic, space group C2 (No. 5), with $a=26.389$ (3), $b=12.942$ (1), $c=11.825$ (1) Å, $\beta=111.22$ (1)°, $V=3964.7$ (8) Å³, $Z=4$, and $D_{\text{calc}}=1.58$ g cm⁻³. Two Rh(II) centers are bridged by four AcO⁻ groups in the $\eta^1:\eta^1$ mode across a Rh-Rh single bond, and octahedral coordination at Rh(1) and Rh(1') is completed by axially coordinating (*S,R*)-CPFA and a bridging AcO⁻, respectively.

Introduction

Dimeric rhodium(II) complexes^{1,2}, notably those with bridging carboxylate ligands³, have been the subject of considerable study in the past two decades. Their interesting structural and spectroscopic properties, along with observed catalytic⁴, and antitumor activities⁵, have led to numerous investigations of the rhodium-rhodium and rhodium-ligand interactions. These complexes contain a rhodium-rhodium single bond with four equatorial bridging carboxylate ions, which are relatively inert to substitution⁶. The two axial positions may be occupied by donor solvents that can undergo rapid ligand exchange to yield adducts with a variety of ligand species³. In this connection, much attention has recently been focused on the nature of the rhodium-ligand bonding interactions, *i.e.*, cyclometallation reaction.⁷⁻¹³

As part of our ongoing project on the synthesis and application of rhodium complexes incorporating ferrocene-containing ligands in homogeneous catalysis¹⁴, we have prepared some ferrocenylphosphines including those new series of aminoferrocenes **3**, **4**, **6**, and **7** described in Schemes 1 & 2 and their dirhodium acetate complexes **8-10** to investigate not only the coordination behavior of these ligands with $\text{Rh}_2(\text{OAc})_4(\text{MeOH})_2$ but catalytic potentiality of the resulting complexes. One such area would be asymmetric cyclopropanation¹⁵⁻¹⁹ as represented by equation (1).

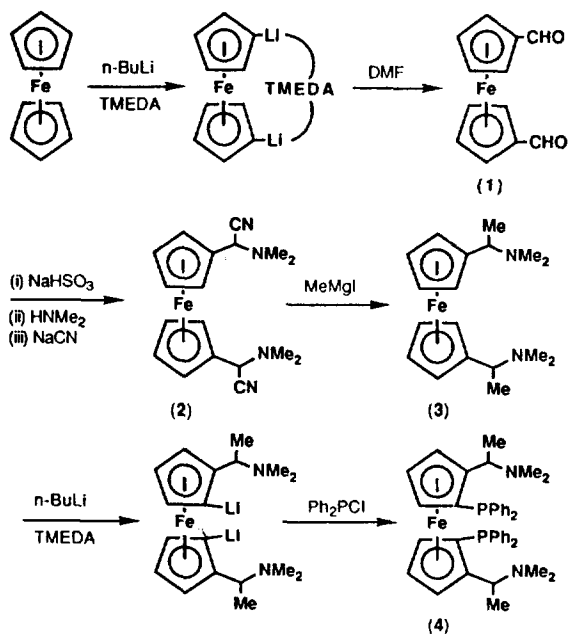
In this paper are described the synthesis and structural



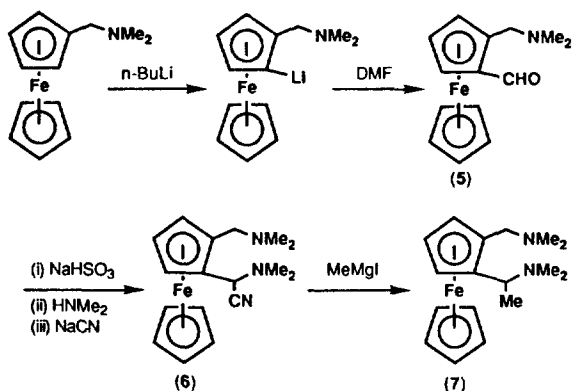
characterization of these new ferrocene-based ligands. Also are described the reaction and coordination chemistry of $\text{Rh}_2(\text{OAc})_4$ with the ligand **4** and other related compounds BPPF and CPFA as presented in Scheme 3.

Experimental

Reagent and Instruments. All manipulations were carried out under an argon atmosphere using a double manifold vacuum system and Schlenk techniques. All commercial reagents were used as received unless otherwise mentioned. Solvents were purified by standard methods¹⁹, and were freshly distilled prior to use. Microanalyses were performed by The Center for Instrumental Analysis, Kyungpook National University. ¹H and ³¹P NMR spectra were recorded on a Bruker AM-300 spectrometer operating at 300 and 121.5 MHz, respectively. ¹H shifts are reported relative to external TMS ($\delta=0$ ppm) and ³¹P shifts relative to 85% H₃PO₄. IR spectra were recorded on a Mattson FT-IR Galaxy 6030E. Melting points were determined using Thomas-Hoover melting point apparatus and reported without correction. The



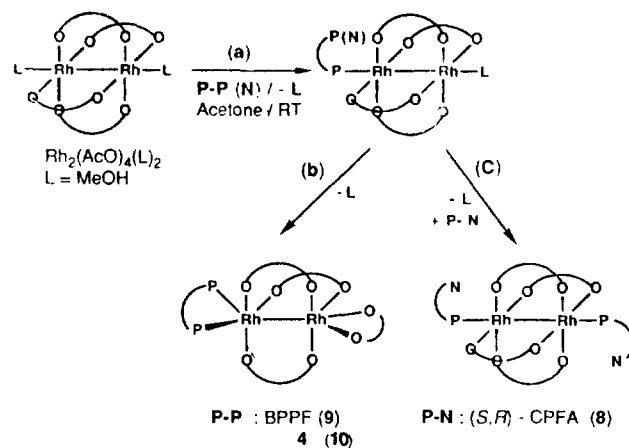
Scheme 1.



Scheme 2.

ligands BPPF and (*S,R*)-CPFA were prepared and resolved as reported previously.²⁰⁻²⁴

X-ray crystallographic analysis of (η^1 -(*S,R*)-CPFA-*P*)₂Rh₂(OAc)₄ (8). Crystal of **8** was grown at room temperature from a hexane/acetone solution of the compound. The crystal, 0.10 × 0.14 × 0.16 mm, was mounted in a capillary on an Enraf-Nonius CAD-4 diffractometer, and lattice parameters were determined by least-squares analysis of 25 reflections. Data were collected with graphite-monochromated MoK α ($\lambda = 0.71073$ Å) by using the $\omega/2\theta$ scan mode. The intensity standard were monitored every 1 h during data collection. The data were modified for Lorentz-polarization effects and decay. Empirical absorption correction with ψ -scans was applied to the data. The structure was solved by use of the conventional heavy-atom method as well as Fourier difference techniques and refined on F by means of full-matrix least-squares procedures using Molen. All non-hydrogen atoms except for hydrogen atoms were refined anisotropically. The final cycle of refinement converted with $R = 0.050$ and $R_w = 0.071$, where ω is $1/[(\sigma(I)^2 + (\phi F_o^2))^{1/2} 2F_o]^2$. The shift/esd ratio in the last cycle of least-squares is less



Scheme 3.

than 0.08 for all parameters. Crystal data, details of the data collection, and refinement of the structure are listed in Table 4. Final positional parameters and temperature factors are listed in Table 3.

Synthesis of Ferrocene-1,1'-dicarboxaldehyde (1).

Ferrocene-1,1'-dicarboxaldehyde was prepared as reported previously with slight modification.²⁵ Ferrocene (5.0 g, 26 mmol) in dry ether (60 mL) was treated with 1.6 M *n*-butyllithium (35.3 mL, 56 mmol) in hexane, and subsequent addition of *N,N,N',N'*-tetramethylethylenediamine (TMEDA) (8.5 mL, 56 mmol). The reaction mixture was stirred for 20 h, then dimethylformamide (DMF) (6.5 mL) was added dropwise at -78 °C. After stirring 2 h, the mixture was hydrolyzed at -78 °C. The cooling bath was removed, and then warmed to room temperature over a period of 1 h. The organic phase was extracted with CH₂Cl₂ to give a red solution that was applied to column chromatography (silicagel) and the two major product bands were identified by visual inspection. The eluents used were mixtures of hexane and diethyl ether or CH₂Cl₂ in increasing polarity throughout the separation. The first band of ferrocenecarboxaldehyde was eluted using a mixture of hexane/diethyl ether (1/1), and the second band of ferrocene-1,1'-dicarboxaldehyde using a mixture of diethyl ether/CH₂Cl₂ (1/1). The first product was crystallized from hexane/diethyl ether (1/2) to give ferrocenecarboxaldehyde as orange-red solid (0.87 g, 15%). The second product crystallized from cyclohexane was identified to be ferrocene-1,1'-dicarboxaldehyde as shiny red crystals (4.6 g, 70%). mp. 147 °C (decomp); Anal. Calcd. For Fe₁O₂C₁₂H₁₀: C, 59.55; H, 16. Found: C, 59.40; H, 3.90.

Synthesis of 2. This new compound was prepared essentially by employing the preparative method for its mono derivatives.²³ Ferrocene-1,1'-dicarboxaldehyde (4 g, 16.5 mmol) dissolved in methanol (20 mL) was added at room temperature to a stirred solution of sodium bisulfite (3.9 g, 37 mmol) in water (20 mL) in a 500 mL, round-bottom flask. After stirring 30 min, a solution of dimethylamine (4.7 mL, 37 mmol) in water (40% wt) was added to the above mixture, followed by a solution of sodium cyanide (1.8 g, 37 mmol) in water (8 mL). The color changed from dark-red to brown-red. Ether (35 mL) was added and the reaction mixture was stirred overnight, then extracted with excess ether. The combined ethereal extracts were dried over K₂CO₃, and the sol-

vent was removed under vacuum. The residual amber oil was recrystallized from CH_2Cl_2 /hexane. The yellow solid (**2**) obtained was washed with hexane and dried under vacuum (3.9 g, 68%). mp. 136 °C; Anal. Calcd. For $\text{Fe}_1\text{N}_4\text{C}_{18}\text{H}_{22}$: C, 61.70; H, 6.33; N, 15.99. Found: C, 61.40; H, 6.14; N, 15.94.

Synthesis of 3. A solution of **2** (3.3 g, 9.4 mmol) in dry ether (20 mL) was added dropwise, through a pressure equalizing dropping funnel, to a solution of MeMgI prepared from methyl iodide (2.4 mL, 37.7 mmol) and Mg (0.8 g, 34.3 mmol) in ether (25 mL) in a 500 mL, round-bottom flask. The yellowish brown color of the aminonitrile changed to reddish orange. The reaction mixture was stirred overnight and slowly treated with aq. NH_4Cl . The ethereal layer was separated and the aqueous layer extracted with excess ether. The combined ethereal extracts were dried over K_2CO_3 , and ether removed at a reduced pressure to give an amber oil (1.5 g, 49%).

Synthesis of 4. The compound **3** (1 g, 3.1 mmol) was dissolved in dry ether (3 mL) in a Schlenk tube. To this solution was added *n*-BuLi (1.6 M, 5.3 mL) in hexane. The suspension was rapidly stirred, and freshly distilled TMEDA (1 g, 8.5 mmol) was added slowly to give a deep cherry solution. After stirring 8 h, Ph_2PCl (1.5 g, 8.5 mmol) was added dropwise through a pressure equalizing dropping funnel. The reaction mixture was stirred overnight. Following careful hydrolysis with aqueous sodium bicarbonate, the organic layer was separated, dried over K_2CO_3 , filtered, and the resulting orange-red solution was evaporated to dryness. The oily residue was recrystallized from EtOH/ether (1/1). The orange crystals obtained were washed with EtOH and dried under vacuum (0.23 g, 11%). mp. 196 °C; Anal. Calcd. For $\text{Fe}_1\text{P}_2\text{N}_2\text{C}_{42}\text{H}_{46}$: C, 72.40; H, 6.65; N, 4.000. Found: C, 72.10; H, 6.61; N, 3.60.

Synthesis of 5. *N,N*-dimethylaminomethylferrocene (5 g, 20.6 mmol) in dry ether (55 mL) was treated with *n*-butyllithium (1.6 M, 15.6 mL) in hexane. The reaction mixture was stirred for 6 h, and dry DMF (5.2 mL) was added dropwise at -78 °C. The color changed from orange-red to brown while the reaction mixture was stirred overnight. The mixture was hydrolyzed at -78 °C. The cooling bath was removed, and then warmed to room temperature over a period of 1 h. The organic phase extracted with CH_2Cl_2 , dried over MgSO_4 , and the solvent removed at a reduced pressure to give a red oil (7 g, 93%).

Synthesis of 6. A solution of **5** (6.3 g, 23.1 mmol) in methanol (25 mL) was added at room temperature to a stirred solution of sodium bisulfite (2.7 g, 25.8 mmol) in water (14 mL) in a 500 mL, round-bottom flask. After stirring 1 h, a solution of dimethylamine (3.2 mL, 25.8 mmol) in water (40% wt) was added to the above mixture, followed by a solution of sodium cyanide (1.2 g, 23.1 mmol) in water (6 mL). The color changed from red to brown. Ether (30 mL) was added and the reaction mixture was stirred overnight, then extracted with excess ether. The combined ethereal extracts were dried over K_2CO_3 , and solvent removed at a reduced pressure to give an amber oil (2.8 g, 34%).

Synthesis of 7. A solution of **6** (2.8 g, 8.7 mmol) in dry ether (13 mL) was added dropwise, through a pressure equalizing dropping funnel, to a solution of MeMgI prepared from methyl iodide (2 mL, 19 mmol) and Mg (0.42 g, 17.4 mmol) in ether (20 mL) in a 500 mL, round-bottom flask.

The yellowish brown color of the aminonitrile changed to orange. The reaction mixture was stirred overnight and slowly treated with aq. NH_4Cl . The ethereal layer was separated and the aqueous layer extracted with excess ether. The combined ethereal extracts were dried over K_2CO_3 , and ether removed at a reduced pressure to give an amber oil (1.8 g, 55%).

Synthesis of 8-10. These were prepared typically as follows. An aqua-blue slurry of $\text{Rh}_2(\text{OAc})_4(\text{MeOH})_2$ ²⁶ (30.3 mg, 0.06 mmol) in acetone (10 mL) was treated with a solution of one or one and half molar amount of corresponding ligands in acetone (5 mL), and stirred at room temperature for 10 min to give precipitates. The solid was isolated by filtration, washed copiously with acetone, dried in vacuum, and recrystallized from acetone/hexane (3/1).

Yield of **8**: (0.023 g, 29%). red solid; mp. 170 °C (decomp); Anal. Calcd. For $\text{Rh}_2\text{Fe}_2\text{P}_2\text{O}_8\text{N}_2\text{C}_{60}\text{H}_{92}$: C, 53.43; H, 2.10; N, 6.83. Found: C, 53.79; H, 2.56; N, 6.88.

Yield of **9**: (0.021 g, 35%). orange solid; mp. 192 °C (decomp); Anal. Calcd. For $\text{Rh}_2\text{Fe}_1\text{P}_2\text{O}_8\text{C}_{42}\text{H}_{40}$: C, 50.65; H, 4.02. Found: C, 50.49; H, 4.04.

Yield of **10**: (0.023 g, 33%). red solid; mp. 185 °C (decomp); Anal. Calcd. For $\text{Rh}_2\text{Fe}_1\text{P}_2\text{O}_8\text{N}_2\text{C}_{50}\text{H}_{58}$: C, 52.70; H, 5.10; N, 2.46. Found: C, 52.63; H, 5.14; N, 2.48.

Results and Discussion

Ferrocene-Containing Chelate Ligands. Schemes 1 and 2 show the synthetic routes leading to the formation of a series of chiral bidentate ferrocenylamines (**3** and **7**) and a potential tetradentate aminophosphine (**4**). The key intermediates mono- and bis-ferrocenecarboxaldehydes, **1** and **5**, in both schemes are easily prepared by treating the corresponding lithioferrocenes with DMF as described by Balavoine *et al.*²⁵ The TMEDA adduct of 1,1'-dilithioferrocene may be used either *in situ* or separated as an pyrophoric powder for further reactions. There are, however, distinct advantages in using the isolated product in order to guarantee the maximum yield of **1** with the reduced amount of the monoaldehyde derivative. As for the formation of the racemic chiral aminoaldehyde (**5**), the lithioaminoferrocene was used *in situ*.

The next step essentially employs the well-known procedure developed by Lindsay²³ for the preparation of the chelate bidentate amines **3** and **7**. Although the resolution of these chiral amines was not conducted at this stage the ligand **3** may be obtained in principle as a pair of enantiomers (*R,R*)- and (*S,S*)-**3** by simple modification of Ugi's procedures²² for the resolution of *N,N*-dimethylethylferrocene, abbreviated as FA. Stepwise lithiation of **3** followed by treatment with chlorophenylphosphine resulted in **4** as an air-stable orange solid.

It can be seen from Schemes 1 and 2 that mono- and bis-ferrocenecarboxaldehydes may serve as very versatile starting compounds for the preparation of a variety of ferrocene-containing derivatives

The formation of all these ligands have been confirmed by spectroscopic data listed in Table 1. The ¹H NMR patterns for the racemic chiral ligands **2**, **3**, and **4** are as expected. For instance, they give rise to the characteristic singlets for the - NMe_2 protons at 2.27, 1.98, and 1.55 ppm, respectively.

Table 2. Crystal Data, Data Collection, and Refinement of the structure for **8**

formula	Rh ₂ Fe ₂ P ₂ O ₈ N ₂ C ₆₀ H ₉₂
fw	1347.59
space group	C2 (No. 5)
a, Å	26.389 (3)
b, Å	12.942 (1)
c, Å	11.825 (1)
β, °	111.22 (1)
V, Å ³	3964.7 (8)
Z	4
D _{calc.} (g·cm)	1.58
crystal size, mm	0.10×0.14×0.16
μ (MoKα), cm ⁻¹	31.99
scan method	ω/2θ
data collected	5858
range of data collection	<i>h</i> , - <i>h</i> , ± 1; 2.61 ≤ 2θ ≤ 30.44°
no. of unique data ≥ 3σ (1)	4505
no. of parameters refined	343
R = Σ (F _o - F _c) / Σ F _o	0.050
Rω = Σ ω ^{1/2} (F _o - F _c) / Σ ω ^{1/2} F _o	0.071

$$\omega = 1 / ((\sigma(F_o))^2 + (\sigma(F_c))^2) / 2F_o^2$$

Table 3. Final positional parameters and *B*_{eq} temperature factors^a for **8**

Atom	<i>x</i>	<i>y</i>	<i>z</i>	<i>B</i> _{eq} (Å ²) ^b
RH1	0.04543(2)	-0.001	0.57970(4)	2.316(8)
FE1	0.19486(4)	-0.23235(9)	0.77408(9)	2.88(2)
P1	0.13748(6)	0.0173(1)	0.7537(1)	2.21(3)
O1	0.0164(2)	-0.1048(5)	0.6699(4)	3.5(1)
O2	0.0186(2)	0.1171(5)	0.6558(5)	3.5(1)
O3	0.0687(2)	0.0988(5)	0.4743(4)	3.1(1)
O4	0.0640(2)	-0.1207(4)	0.4857(4)	3.0(1)
N1	0.2213(2)	0.0197(5)	0.5435(5)	3.2(1)
C1	0.1939(3)	-0.0741(5)	0.7786(6)	2.5(1)
C2	0.2285(3)	-0.1162(6)	0.8950(6)	3.0(2)
C3	0.2702(3)	-0.1758(7)	0.8769(8)	3.8(2)
C4	0.2610(3)	-0.1732(7)	0.7481(7)	3.6(2)
C5	0.2144(3)	-0.1083(6)	0.6874(6)	2.8(1)
C6	0.1181(4)	-0.2848(7)	0.7435(9)	4.6(2)
C7	0.1548(4)	-0.3260(8)	0.8574(8)	4.7(2)
C8	0.1949(4)	-0.3837(7)	0.8269(9)	5.2(3)
C9	0.1825(4)	-0.3775(7)	0.6936(8)	4.5(2)
C10	0.1355(4)	-0.3141(8)	0.6466(8)	4.6(2)
C11	0.1365(3)	0.0254(6)	0.9112(5)	2.7(1)
C12	0.1054(4)	0.1186(8)	0.9303(7)	5.0(2)
C13	0.1083(4)	0.1205(9)	1.0677(7)	5.6(2)
C14	0.0865(4)	0.0241(9)	1.0980(7)	4.9(2)
C15	0.1141(4)	-0.0737(9)	1.0758(7)	4.9(2)
C16	0.1125(4)	-0.0764(7)	0.9400(7)	4.2(2)
C17	0.1733(3)	0.1372(6)	0.7327(6)	2.7(1)
C18	0.1375(3)	0.2369(6)	0.7014(7)	3.6(2)
C19	0.1688(4)	0.3202(7)	0.6590(8)	4.1(2)
C20	0.2244(4)	0.3434(7)	0.7540(8)	4.3(2)

C21	0.2578(3)	0.2455(7)	0.7935(8)	4.2(2)
C22	0.2281(3)	0.1590(7)	0.8355(7)	3.4(2)
C23	0.1943(3)	-0.0790(6)	0.5572(6)	2.9(1)
C24	0.2021(4)	-0.1670(7)	0.4759(7)	4.0(2)
C25	0.2810(3)	0.0143(9)	0.5719(8)	4.7(2)
C26	0.1945(4)	0.0710(8)	0.4294(8)	4.7(2)
C27	-0.0313(4)	-0.1422(7)	0.6171(7)	3.6(2)
C28	-0.0489(3)	-0.2214(9)	0.6918(7)	5.0(2)
C29	-0.0317(3)	0.1403(6)	0.6188(6)	2.8(1)
C30	-0.0495(4)	0.2218(8)	0.6851(7)	4.6(2)

^aNumbers in parentheses are the estimated standard deviations in the units of the least significant figure given for the corresponding parameter. ^bAnisotropically refined atoms are given in the form of the isotropic equivalent displacement parameter defined as: (4/3) [a²β₁₁ + b²β₂₂ + c²β₃₃ + ab (cos ρ)β₁₂ + ac (cos β)β₁₃ + bc (cos α)β₂₃].

Table 4. Selected Bond Distances (Å) and Angles (deg) for **8**

a. Bonds				
Rh(1)-Rh(1)	2.453(1)	Fe(1)-C(1)	2.049(7)	
Rh(1)-P(1)	2.561(2)	Fe(1)-C(2)	2.042(9)	
Rh(1)-O(1)	2.027(7)	Fe(1)-C(3)	2.05(1)	
Rh(1)-O(1)	3.110(7)	Fe(1)-C(4)	2.028(9)	
Rh(1)-O(2)	2.030(7)	Fe(1)-C(5)	2.068(8)	
Rh(1)-O(2)	3.089(7)	Fe(1)-C(6)	2.04(1)	
Rh(1)-O(3)	2.039(7)	Fe(1)-C(7)	2.08(1)	
Rh(1)-O(3)	3.121(7)	Fe(1)-C(8)	2.056(9)	
Rh(1)-O(4)	2.063(6)	Fe(1)-C(9)	2.08(1)	
Rh(1)-O(4)	3.113(7)	Fe(1)-C(10)	2.03(1)	
				Mean
C-C(ring)	1.42-1.49(2)			1.46
C-C(Cy)	1.48-1.59(1)			1.54
N-C	1.42-1.50(1)			1.46
C(23)-C	1.48, 1.55(1)			1.52
b. Angles				
Rh(1)-Rh(1)-P(1)	173.81(4)	P(1)-Rh(1)-O(4)	99.4(2)	
Rh(1)-Rh(1)-O(1)	84.4(2)	P(1)-Rh(1)-O(4)	140.3(1)	
Rh(1)-Rh(1)-P(1)	40.6(1)	O(1)-Rh(1)-O(2)	92.7(3)	
Rh(1)-Rh(1)-O(2)	86.6(2)	O(1)-Rh(1)-O(2)	90.4(3)	
Rh(1)-Rh(1)-O(2)	41.0(1)	O(1)-Rh(1)-O(2)	128.0(3)	
Rh(1)-Rh(1)-O(3)	87.5(2)	O(1)-Rh(1)-O(3)	174.6(3)	
Rh(1)-Rh(1)-O(3)	40.7(1)	O(1)-Rh(1)-O(3)	82.1(2)	
Rh(1)-Rh(1)-O(4)	86.7(2)	O(1)-Rh(1)-O(4)	89.9(3)	
Rh(1)-Rh(1)-O(4)	41.4(1)	O(1)-Rh(1)-O(4)	46.4(2)	
P(1)-Rh(1)-O(1)	93.9(2)	O(1)-Rh(1)-O(2)	126.8(3)	
P(1)-Rh(1)-O(1)	145.2(1)	O(1)-Rh(1)-O(2)	55.3(2)	
P(1)-Rh(1)-O(2)	87.4(2)	O(1)-Rh(1)-O(3)	82.2(2)	
P(1)-Rh(1)-O(2)	136.6(1)	O(1)-Rh(1)-O(3)	81.4(2)	
P(1)-Rh(1)-O(3)	91.4(2)	O(1)-Rh(1)-O(4)	46.5(2)	
P(1)-Rh(1)-O(3)	133.4(1)	O(1)-Rh(1)-O(4)	55.3(2)	
C-C-C(ring)	105.2-109.7(8)			107.5
C(ring)-P-C(Cy)	98.8-100.3(3)			99.1

to the presence of two different substituents on the same ring.

Iron atom is sandwiched between two cyclopentadienyl rings which are very close to planar, deviate slightly from coplanarity, and are separated by an average of 3.29 Å. The Fe-C bonds (Table 4) fall into two distinct groups; those involving unsubstituted ring atoms are in the range 2.028-2.08 (5), mean 2.054 Å, while for substituted ring atoms the distances are 2.049-2.068 (8), mean 2.059 Å. The slightly longer average distances to the substituted carbon atoms suggest lower electron-density at these positions, particularly at those with phosphine substituents. These bond length variations probably cause the small deviations from ring planarity, the unsubstituted C atoms being displaced slightly toward the Fe atoms. The C-C bond lengths and C-C-C angles in the cyclopentadienyl rings also show some variations. Individual differences cannot be considered significant, but mean C-C lengths are 1.44 Å if the bond involves only unsubstituted C atoms, and 1.45 Å if a substituted atom is involved; corresponding mean C-C-C angles are 108.2° at unsubstituted and 106.8° at substituted C atoms. These variations again suggest lower electron-density at substituted carbon atoms. Bond lengths in the dimethylaminoethyl group are normal, mean C-C 1.52, C-N 1.47 Å.

Two Rh(II) centers are bridged by four AcO⁻ groups in the familiar η¹:η¹ mode across a Rh-Rh single bond distance, 2.453 (1) Å and is slightly shorter than that 2.475 (2) Å found in the previously reported dirhodium(II) complex Rh₂(OAc)₄(bpy).²⁸ Octahedral coordination at Rh (1) and Rh (1') is completed by axially coordinating CPFA and a bridging AcO⁻, respectively. The phosphorus atoms occupy two axial site with the expected same in Rh-P bond length (2.561 (2) Å). Much greater symmetry is observed in the bridging AcO⁻ group at Rh(1) and Rh(1'), which is an example of a symmetrically-bridging carboxylate. The equatorial disposition of the two oxygen atoms leads to similar Rh-O distances (2.027-2.063 (7)), mean 2.045 Å. The Rh-Rh-P_{axial} angle, 173.81 (4)°, deviates slightly from linearity. This suggests that steric interactions between the bridging carboxylates and the axial ligands are responsible for these deviations.

Unlike the complex **8**, complexes **9**, and **10** are insoluble in most organic solvents. Numerous attempts to obtain solution of complexes **9** and **10** in a form suitable for spectroscopic characterization have all proven unsuccessful. Its identity was thus deduced by other means: namely, elemental analysis indicated retention of the 4:1:2=AcO:ferrocenylphosphine:Rh ratio in **9** and **10**. The methanol bands of starting material Rh₂(OAc)₄(MeOH)₂ are not observed in IR spectra of **9** and **10**. Two ν_{as}(CO) bands (1615, 1594 cm⁻¹) and ν_s(CO) bands (1469, 1428 cm⁻¹) are observed in their IR spectra. The bands at 1615 and 1428 cm⁻¹ are assigned to the bridging AcO⁻ groups and those at 1594 and 1469 cm⁻¹ to the chelating AcO⁻ group.

Acknowledgment. TJK gratefully acknowledges KOSEF and the Ministry of Education (BSRI-94-3403) for the financial support.

References

1. Aquiso, M. A. S.; Macartney, D. H. *Inorg. Chem.* **1987**, *26*, 2696.
2. Felthouse, T. R. *Prog. Inorg. Chem.* **1982**, *29*, 73.
3. Boyar, E. B.; Robinson, S. D. *Coord. Chem. Rev.* **1983**, *50*, 109, and references therein.
4. Cotton, F. A.; Walton, R. A. *Multiple Bonds Between Metal Atoms*; Wiley-Interscience: New York, 1982; Chapter 7, and references therein.
5. Howard, R. A.; Spring, T. G.; Bear, J. L. *Cancer. Res.* **1976**, *36*, 4402.
6. Bear, J. L.; Kitchens, J.; Willcott, M. R. *J. Inorg. Nucl. Chem.* **1971**, *33*, 3479.
7. Cotton, F. A.; Barcelo, F.; Lahuerta, P.; Lluser, R.; Paya, J.; Ubada, M. A. *Inorg. Chem.* **1988**, *27*, 1010.
8. Lahuerta, P.; Paya, J.; Peris, E.; Pellinghelli, M. A.; Tiripicchio, A. *J. Organomet. Chem.* **1989**, *373*, C5-C7.
9. Lahuerta, P.; Paya, J.; Bianchi, A. *Inorg. Chem.* **1992**, *31*, 5336.
10. Lahuerta, P.; Paya, J.; Pellinghelli, M. A.; Tiripicchio, A. *Inorg. Chem.* **1992**, *31*, 1224.
11. Lahuerta, P.; Paya, J.; Solans, X.; Ubada, M. A. *Inorg. Chem.* **1992**, *31*, 385.
12. Lahuerta, P.; Peris, E.; Ubada, M. A.; Garcia-Granda, S.; Gomez-Beltran, F.; Diaz, M. R. *J. Organomet. Chem.* **1993**, *455*, C10-C12.
13. Lahuerta, P.; Paya, J.; Garcia-Granda, S.; Gomez-Beltran, F.; Anillo, A. *J. Organomet. Chem.* **1993**, *443*, C14-C15.
14. Kim, T. J.; Lee, K. C. *Bull. Korean Chem. Soc.* **1989**, *10*, 279.
15. (a) Doyle, M. P. *Chem. Rev.* **1986**, *86*, 919. (b) Mass, G. *Top. Curr. Chem.* **1987**, *137*, 75.
16. (a) Hubert, A. J.; Noels, A. F.; Teyssie, P. *Synthesis*. **1976**, 600. (b) Anciaux, A. J.; Hubert, A. J.; Noel, A. F.; Petinot, N.; Teyssie, P. *J. Org. Chem.* **1980**, *45*, 695.
17. Doyle, M. P.; Dorow, R. L.; Buhro, W. E.; Griffine, J. H.; Tamblyn, W. H.; Trudell, M. L. *Organometallics* **1984**, *3*, 44.
18. Doyle, M. P. *Acc. Chem. Res.* **1986**, *19*, 348.
19. Perrin, D. D.; Armarego, W. L. F. *Purification of Laboratory Chemicals*; 3rd edition; Pergamon Press, 1988.
20. Bishop, J. J.; Davison, A.; Katcher, M. L.; Lichtenberg, D. W.; Merrill, R. E.; Smart, J. C. *J. Organomet. Chem.* **1971**, *27*, 241.
21. Kim, T. J.; Kim, Y. H.; Kim, H. S.; Shim, S. C.; Kwak, Y. W.; Cha, J. S.; Lee, H. S.; Uhm, J. K.; Byun, S. I. *Bull. Korean Chem.* **1992**, *13*, 588.
22. (a) Marquarding, D.; Klusacck, H.; Gokel, G.; Hoffman, P.; Ugi, I. *J. Am. Chem. Soc.* **1970**, *92*, 5389. (b) Gokel, G.; Ugi, I. *J. Chem. Educ.* **1972**, *49*, 294.
23. Hauser, C. R.; Lindsay, J. K. *J. Org. Chem.* **1957**, *22*, 906.
24. Hayashi, T.; Mise, T.; Fukushima, M.; Katagoni, M.; Nagashima, M.; Hamada, Y.; Matsumoto, A.; Kawakami, S.; Konishi, M.; Kumada, M. *Bull. Chem. Soc. Jpn.* **1980**, *53*, 1138.
25. Balavoine, G. G. A.; Doisneau, G.; Fillebeen-Khan, T. J. *Organomet. Chem.* **1991**, *412*, 381.
26. Rempel, G. A.; Legzdins, P.; Smith, H.; Wilkinson, G. *Inorg. Synth.* **1972**, *13*, 90.
27. Cullen, W. R.; Einstein, F. W. B.; Jones, T.; Kim, T. J. *Organometallics* **1983**, *2*, 741.
28. Crawford, C. A.; Matonic, J. H.; Streib, W. E.; Huffman, J. C.; Dunbar, K. R.; Chirstou, G. C. *Inorg. Chem.* **1993**, *32*, 3135.

29. Kim, T. J.; Kwon, S. C.; Kim, Y. H.; Heo, N. H. *J. Organomet. Chem.* **1992**, 426, 71.
 30. Hor, T. S. A.; Phang, L. T. *J. Organomet. Chem.* **1989**,

- 373, 319.
 31. Morrison, E. C.; Tocher, D. A. *J. Organomet. Chem.* **1991**, 408, 105.

Theoretical Studies of d^0 Titanocene Complexes

Sung Kwon Kang*, Byeong Gak Ahn, and Eun Suk Choi

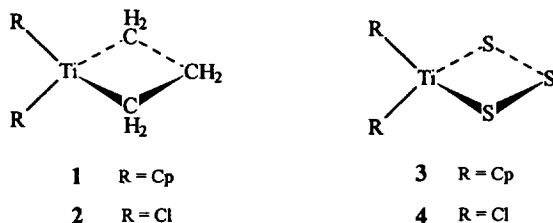
Department of Chemistry, Chungnam National University, Taejeon 305-764, Korea

Received August 10, 1994

Ab initio calculations with various basis sets have been carried out to investigate the geometries and ring inversion barrier of $R_2TiC_3H_6$ and R_2TiS_3 , $R=Cp$ and Cl . Optimized geometries of $R_2TiC_3H_6$ showed the four membered ring was planar on C_2 symmetry. However, R_2TiS_3 complexes were optimized to be stable in the puckered form. The smallest Basis III with STO-3G on Cp ligands gave reasonable results for the calculations of metallocene. The energy barrier for the ring inversion of metallacyclosulfanes, Cp_2TiS_3 was computed to be 8.72 kcal/mol at MP2 level. For the Cl system, we reproduced the molecular structure and ring inversion energy with Basis V.

Introduction

The electronic structures and bonding properties of transition metal complexes are not as well understood as organic molecules are. The elementary reaction steps with transition metal complexes have been studied by various theoretical methods such as the semi-empirical and ab initio calculations. Quantitative ab initio calculations on transition metal complexes are only recently becoming commonplace due to the large number of electrons and poor basis sets. Several approaches are available to investigate the large transition metal complexes. For instance, effective core potentials (ECP),¹ density functional theory (DFT),² and model systems³ with all electron calculations are useful methods. We have started to investigate systematically the performance of model system calculations. $Cp_2TiC_3H_6$ (**1**), $Cl_2TiC_3H_6$ (**2**), Cp_2TiS_3 (**3**), and Cl_2TiS_3 (**4**) complexes have been chosen to study the substitution effect of cyclopentadienyl (Cp) ligand by Cl ligand in theoretical viewpoint.



The Cp ligand is ubiquitous in transition metal complexes. Titanium-cyclopentadienyl complexes shows the rich structural chemistry of Cp ligand⁴ and are also important in a number of synthetic applications. It is known that the geometry and properties of Cp ligand in Cp_2TiCl_2 and its derivatives are useful to cancer research.⁵ Dicyclopentadienyltitanacyclobutane (**1**) is considered to be one of the important intermediates in Ziegler-Natta catalytic systems. In 1978, Green and Rooney⁶ proposed a metathesis type mechanism in studies

Table 1. Ligand Basis Sets Used in This Study

Basis Sets	No. of basis functions	
	$Cp_2TiC_3H_6$ or Cl_2TiS_3	$Cl_2TiC_3H_6$ or Cl_2TiS_3
I C (Cp); 3-21G, H (Cp); STO-3G C, H (C_3H_6), S; 4-31G	164	
II C (Cp); 3-21G, H (Cp); STO-3G C, H (C_3H_6), S; 4-31G*	182	
III C, H (Cp); STO-3G C, H (C_3H_6), S; 4-31G*	142	
IV ^a C, H (C_3H_6), Cl, S; 4-31G		90
V ^a C, H (C_3H_6), Cl, S; 4-31G*		120

^aBasis Sets for model systems of $Cl_2TiC_3H_6$ and Cl_2TiS_3

of the stereospecific Ziegler-Natta polymerization reaction of olefins. Complex **3** (metallacyclosulfane) is isoelectronic with complex **1**. We recently⁷ examined the electronic structures and four-membered ring inversion motion with the extended Hückel and preliminary ab initio calculations. In this publication, molecule structures and inversion process of four-membered ring shall be examined for **1-4** complexes using all electron ab initio molecular orbital theory with various basis sets.

Computational Methods

The ab initio calculations were carried out with the GAUSSIAN 92⁸ and GAMESS⁹ on a Cray Y-MP C916 and an IBM, respectively. The basis set for Ti metal atom was of the form (4333/433/31) and has been described elsewhere.¹⁰ Basically, it is of double- ξ quality for the metal d region. Table 1 shows the combinations of ligand basis sets used in this study.

Table 1. NME (^1H & ^{31}P) Data for **2-8**^{a,b}

Compound	^1H	^{31}P
2	1.65 (s, CH, 2H), 2.27 (s, NMe ₂ , 12H), 4.32-4.74 (m, A ₂ B ₂ , 8H, Cp)	
3	1.35 (d, Me, 6H, $J_{\text{HH}}=3$), 1.98 (s, NMe ₂ , 12H), 3.48 (q, CH, 2H, $J_{\text{HH}}=3$), 4.04-4.25 (m, A ₂ B ₂ , 8H, Cp)	
4	0.45 (d, Me, 6H, $J_{\text{HH}}=6.7$), 1.55 (s, NMe ₂ , 12H), 3.62-4.23 (m, ABC, 6H, Cp), 7.07-7.60 (m, 20H, pH)	-23.5 (s)
5	2.27 (s, NMe ₂ , 6H), 3.47 (q, CH ₂ , $J_{\text{HH}}=13$), 4.23 (s, 5H, Cp), 4.45-4.57 (m, 3H, Cp), 10.09 (s, CHO, 1H)	
6	1.36 (s, CH, 1H), 2.28 (s, NMe ₂ , 6H), 2.31 (s, NMe ₂ , 6H), 2.97 (bs, CH ₂ , 2H), 4.13 (s, Cp, 5H), 4.06-4.70 (m, 3H, Cp)	
7	1.51 (d, Me, 3H, $J_{\text{HH}}=3$), 2.16 (s, NMe ₂ , 6H), 2.23 (s, NMe ₂ , 6H), 2.90 (q, CH ₂ , $J_{\text{HH}}=13$), 3.54 (q, CH, 1H, $J_{\text{HH}}=7$), 4.04-4.11 (m, 3H, Cp), 4.06 (s, 5H, Cp)	
8	1.18 (d, Me, 6H, $J_{\text{HH}}=7$), 1.23-1.68 (m, Cy, 44H), 1.86 (s, AcO, 12H), 2.16 (s, NMe ₂ , 12H), 3.44 (q, CH, 2H, $J_{\text{HH}}=13$), 4.20 (s, 10H, Cp), 4.25-4.38 (m, 6H, Cp)	-13.4 (m) -22.6 (m)

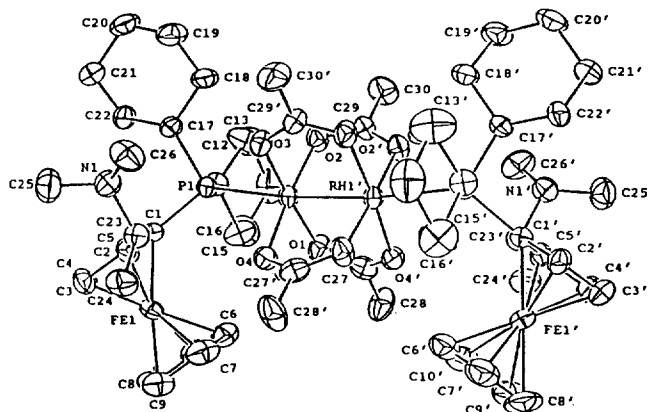
^aAll Spectra were recorded in CDCl₃. ^bCoupling constants are in Hz: s=singlet, bs=broad singlet, d=doublet, m=multiplet, q=quartet. The methine proton is obscured by the Cp ring protons.

These signals arise due to the free rotation along the bond connecting the nitrogen and asymmetric carbon. The methyl groups on the chiral center exhibit doublets at 1.35 and 0.45 ppm for **3** and **4**, respectively, as a result of coupling with the geminal methine protons ($J_{\text{HH}}=3$ Hz). The signal due to the methine proton in the compound **4** is obscured by overlapping with one of the Cp ring protons at 3.77 ppm. The ^{31}P NMR signal for the equivalent pair of the -PPh₂ moiety in **4** appears at -17.61 ppm.²⁷

Two other amine derivatives **6** and **7** exhibit a common ^1H NMR pattern; that is, a pair of singlets due to the diastereotopic pair of -NMe₂ groups. The methylene protons in **7** show almost an AX pattern making one of the protons in the pair appear much further downfield ($\delta=3.61$ and 2.91 ppm) than usually found, while the same protons in **6** show a broad singlet at 2.97 ppm. Other ^1H NMR features are as expected from their structures.

Dirhodium(II) Complexes of Ferrocenylphosphines. As mentioned in introduction one of our research objectives was to investigate the reaction and the coordination chemistry of ferrocenylphosphines with dirhodium(II) tetraacetate.

Scheme 3 shows two different synthetic routes leading to the formation of a series of dirhodium(II) carboxylates (**8-10**) incorporating the ferrocenylphosphines depending upon the choice of the ligands. Namely, the chelating diphos-

**Figure 1.** The X-ray Crystal Structure of **8**.

phine ligands BPPF and **4** form the expected chelation products **9** and **10**, respectively, whose reaction pattern has also been observed with bipyridine.²⁸ The route involves initially the nucleophilic displacement of one methanol by the ligand (step **a**) followed by successive removal of the second methanol by one of the carboxylate oxygen. The vacant site left on one rhodium center is now filled by the second phosphorus in the ligand BPPF or **4** (step **b**). Here it is interesting to note that these symmetrical bidentate ligands do not favor the bimonodentate fashion which has been observed with compounds such as (η^1, η^1 -BPPF)[Fe(CO)₄]₂²⁹ and (η^1, η^1 -BPPF)Mo₂(CO)₁₀.³⁰

In contrast, the chiral analogue (*S,R*)-CPFA serves as a monodentate through phosphorus to each rhodium metal to give (η^1 -*S,R*)-CPFA-*P*)Rh₂(OAc)₄ (**8**) rather than the chelate PN dirhodium complex of the type (η^2 -*S,R*)-CPFA-*P,N*)Rh₂(OAc)₄, replacing one of the phosphoruses in **9** and **10** with the NMe₂ group in the ligand CPFA. The differences in the coordination mode between CPFA and BPPF and **4** seem to lie in the fact that the soft rhodium (II) center still prefers phosphorus which is a stronger nucleophile than nitrogen. The formation of **8** involves two successive replacement of methanol with two equivalents of the CPFA ligand as shown in the scheme (step **c**).

The formation of **8** can be confirmed by its spectroscopic data listed in Table 1. For instance, the ^1H NMR shows a single resonance at 1.86 ppm which is attributed to the four equivalent AcO⁻ groups. The axially coordinated phosphines appear in the ^{31}P NMR as two complex multiplets at -13 and -23 ppm rather than the AA'XX' pattern expected for the solid-state structure. The complex ^{31}P NMR pattern of this sort has also been reported by others for the related dirhodium-phosphine derivatives.³¹ The carboxylate groups give rise to two strong ν (CO) bands at 1598 cm⁻¹ (ν_s) and 1426 cm⁻¹ (ν_{as}).

In order to garner more structural information about **8**, x-ray crystallographic studies have been carried out, and the ORTEP plot of the complex is presented in Figure 1.

Crystallographic data, selected bond distances and angles, and other positional and thermal parameters are listed in Tables 2-4.

The molecule of (*S,R*)-CPFA is chiral, and the analysis has shown an *S* configuration for the amine-substituted C(23) atom, and the second *R* refers to the planar chirality due